International Journal of Hydrogen Energy 160 (2025) 150559

Contents lists available at ScienceDirect

International Journal of Hydrogen Energy

journal homepage: www.elsevier.com/locate/he

Optimized hybrid energy systems for sustainable net-zero communities: Modelling, framework design and performance analysis

K. Parvin [a], Abbas Tabandeh [a,*], M.J. Hossain [a], M.A. Hannan [b,c]

[a] School of Electrical and Data Engineering, University of Technology Sydney, 15 Broadway Sydney, NSW, 2007, Australia
[b] School of Engineering and Technology, Sunway University, Bandar Sunway, Petaling Jaya, 47500, Malaysia
[c] School of Electrical Engineering, Korea University, Seongbuk-Gu, Seoul, 136-701, South Korea

ARTICLE INFO

Handling Editor: Prof. J. W. Sheffield

Keywords:
Techno-economic
Hybrid renewable energy system
Net zero energy
Greenhouse gas emission
Electric vehicle
Hydrogen vehicle

ABSTRACT

Identifying a cost-effective pathway to achieve net zero energy in remote Australian communities is crucial for meeting the country's net zero target by 2050. Hybrid Renewable Energy Systems (HRES) offer a sustainable and economical alternative to traditional power sources by lowering capital costs and improving renewable energy efficiency. This paper presents a sustainable HRES modelling and theoretical framework for designing and optimizing net-zero communities with emerging energy technologies. It examines a PV-Wind hybrid system with various storage technologies to meet energy demands in remote areas of Broken Hill, New South Wales, Australia. Multiple future scenarios are evaluated based on technical, economic, and environmental criteria. The results show that the hybrid system, consisting of PV, wind, battery and hydrogen energy, is the most viable, achieving net zero energy (NZE) with a cost of energy (COE) of $0.0957/kWh and zero CO_2 emissions. The results obtained over time underscore that COE, carbon emission reduction and renewable integration play a crucial role in sustainable energy development and economic growth enhancing energy security and lowering operational costs. Overall, this study highlights the potential of optimized HRES configurations for diverse locations and climates, supporting Australia's transition to a cleaner, more sustainable energy future.

1. Introduction

Energy consumption has increased significantly in recent years as the globe is going through constant economic development toward improving survival standards. About 65 % of energy is still supplied by conventional resources in Australia [1]. Conventional energy sources can meet the electricity demand; however, they have several disadvantages, such as harmful gas emissions and a high life cycle fuel cost. Renewable energy sources (RES) provide a sustainable way to meet power demand and cut emissions. Hybrid PV-wind systems with storage enhance reliability and support rural electrification. Their integration reduces dependence on fossil fuels and promotes cleaner energy solutions. This approach helps achieve net zero emissions (NZE) and long-term energy sustainability. Since these hybrid systems can produce consistent and economical energy, their installation as well as research are getting growing interest [2]. Fast-tracking rural electrification also appears to be an effective way of decreasing carbon dioxide emissions. Currently, electricity generation from PV and wind technologies is one of the leading RES [3]. Zhang et al. [4] deduced that incorporating PV and wind energy may help reduce CO_2 emissions. Moreover, combining RES with energy storage systems (ESS) is thus potentially a good way to improve the consistency of RES due to its variability [5]. Presently, electrochemical energy storage systems come into prominence; examples include lithium and lead-acid (LA) batteries [6]. Such electrochemical ESS are not appropriate for long-term storage required by RES, as it is economically viable only for short-term storage. Also, the hydrogen storage system is the most popular substitute available today since it is environmentally beneficial and does minimum harm to the environment.

Abbreviations

BESS	battery energy storage system	N_{hub}	hub height (m)
CRF	Capital recovery factor	N_{Bat}	Number of batteries
DG	Diesel generator	N_{EZ}	Number of electrolyzers
DoD	Depth of discharge.	N_{FC}	Number of fuel cell

(*continued on next page*)

* Corresponding author.
E-mail address: abbas.tabandeh@uts.edu.au (A. Tabandeh).

https://doi.org/10.1016/j.ijhydene.2025.150559
Received 18 April 2025; Received in revised form 14 July 2025; Accepted 16 July 2025
Available online 25 July 2025

(*continued*)

ESS	Energy storage system	N_{PV}	Number of solar panels
EV	Electric vehicle	N_{WT}	Number of wind turbines
FC	Fuel cell	N_{anem}	Anemometer height
GHG	Greenhouse gas emission	N_{pv}	Capacity of the PV [kW]
HOMER	Hybrid optimization model for electric renewable	P_{EZ}	electrolyzer's electrical power
HRES	Hybrid renewable energy systems	P_{ch}	Power charging the battery
HT	Hydrogen tank	P_{distch}	Power discharge from the battery
COE	Cost of energy	$P_{inv,out}$	inverter's output power
Li-ion	Lithium-ion	$P_{rec,out}$	rectifier's output power
LOCH	Levelized cost of hydrogen	p_{rated}	Rated power [kW]
NASA	National aeronautics and space administration	LH_2	Hydrogen load
TNPC	Total net present cost	SOC_{H2}	State of charge of the HT
NZE	Net zero energy	T_{Cell}	PV cell temperature [°C]
PV	Photovoltaic	$T_{Cell,NOCT}$	Nominal operating cell temperature [°C]
REF	Renewable energy fraction	T_{amb}	Ambient temperature [°C]
RES	Renewable energy sources	U_T	Solar radiation (kW/m^2)
TAC	Total annualised cost	v	Wind speed [m/s]
WT	Wind turbine	v_{rated}	Rated speed [m/s]
GHG	Greenhouse gas		
LCE	Life cycle emissions		
		v_{cut-in}	Cut-in speed [m/s]
Nomenclature		$v_{cut-off}$	Cut-off wind speed [m/s]
$Coef_{H_{2,n}}$	Hydrogen tank multiplication factor	**Greek symbols**	
$C_{H_{2-unit}}$	Nominal capacity of the hydrogen tank [kWh]	α_p	Temperature coefficient of power
$P(t)_{DGgenerated}$	Generated power of DG	β	Power law exponent
$P_{DG,rated}$	Rated power the DG	γ_{DG}	Consumption coefficients of DG
E_{ch}	Energy charged into the battery	η_{inv}	inverter's efficiency
E_{distch}	Energy discharged from the battery	η_{rec}	rectifier's efficiency
H_{hub}	Wind speed at the hub height [m/s]	η_c	Panel efficiency
H_{H2}	Heating value of hydrogen fuel [MJ/kg]	η_l	Battery efficiency
H_{anem}	Anemometer height [m/s]	η_{EZ}	Electrolyser efficiency
I_{pv}	Derating factor of PV [%]	η_{FC}	Fuel cell efficiency
i_r	Project lifespan	σ	Self-discharge rate
LH_2	Hydrogen load	$\tau\alpha$	Solar transmittance and absorptance

Optimizing the design of the hybrid renewable energy systems (HRES) is essential to enhance its efficiency, reliability, and capacity to meet external load requirements, while also reducing energy costs, net present cost (NPC), and greenhouse gas (GHG) emissions [7]. Designing an optimized HRES for countryside areas presents several challenges. Factors, for instance, site selection, costs (including installation, operation, and maintenance), load management, reliability, battery aging, environmental impact, and technology availability complicate the process [8]. To tackle these challenges, scholars have proposed several models and optimization techniques aimed at improving system efficiency.

Several previous studies have modeled and optimized grid-connected HRES, incorporating hydrogen and battery storage options with numerous configurations and methodologies. Dhundhara et al. [9] analyzed a hybrid energy system (HES) combining PV, wind, diesel, and biodiesel with Li-ion and LA batteries in both standalone and grid-connected configurations. Their study found that Li-ion batteries were more technically and economically viable than LA batteries. Another study [10] optimized a grid-associated PV system to minimize costs and enhance reliability by balancing power purchases from the grid and PV system sizing. However, due to high electricity prices in Iran, the PV system was not deemed cost-effective. Another study [11] conducted a bi-objective optimization of a grid-connected HES, including PV, diesel generator (DG), and FC, revealed that lower electricity prices increased the cost of energy (COE) but decreased the grid factor, though the study omitted environmental considerations. This paper [12] proposed an economic model for a grid-related hybrid system combining solar, wind, and FC technologies for residential use. The optimization focused on minimizing operational and maintenance costs, with results showing that such systems are the most economical option for residential energy shortly. Gonzalez A. et al. [13] studied the optimum sizing of a grid-associated hybrid PV-wind system, demonstrating its economic profitability, though without considering energy storage. Ramli M. et al. [14] explored PV system optimization in Saudi Arabia, achieving zero unmet load and reduced CO_2 emissions with an optimal inverter size ratio of R = 1. Reducing the inverter size to 68 % of the PV capacity further lowered system costs. Jahjangiri M. et al. [15] assessed a wind-solar-hydrogen storage system and found an average NPC of $48, 164 and an COE of $0.573/kWh, proposing cost-effective hybrid configurations for electricity and hydrogen production. Akram U. et al. [16] studied a grid-connected wind/solar/battery hybrid microgrid, finding that the optimal configuration was both economical and reduced CO_2 emissions. In Ref. [17], grid-connected and stand-alone hybrid system were the most economical, with an NPC of $28,041 and an energy cost of $0.069/kWh, but it emitted the highest CO_2 levels 26,609 kg/year. Basu et al. [18] compared three configurations using HOMER, identifying the optimal setup as including PV, wind, HS, and a converter, with a COE of $0.3387/kWh.

Despite the significant contributions of previous studies, several research gaps remain unaddressed. For instance, Ma et al. [19] focused solely on a single load profile for a specific site, while Ali and Shahnia [20] analyzed a single load without considering grid connectivity. Similarly, Uddin et al. [21] addressed a single load and storage system for the studied area. Furthermore, these works primarily concentrated on techno-economic and environmental aspects, neglecting sustainability criteria. Crucially, none of these studies considered hydrogen storage system as backup solutions. Sustainability also plays a significant role because global science and technology (S&T) efforts are collaborative initiatives aimed at tackling shared challenges like climate change, health crises, energy transitions, and sustainable development. These efforts span governments, academia, industry, and civil society, and often align with international frameworks such as the UN Sustainable Development Goals (SDGs). Moreover, in Australia, the target is to cut CO_2 emissions by reducing dependence on diesel generators and grid power, while increasing the use of renewable energy sources based on their sustainability projection. This represents a major move towards cleaner energy in the coming decades. To address these limitations, this study conducts a comprehensive analysis of a grid-connected HRES that integrates PV/wind/battery/DG/HT/electrolyser/FC technologies. By adopting a multi-criteria approach, this work evaluates the system's techno-economic, environmental, and sustainability performance for rural electrification in Australia, aiming to deliver an optimized and future-ready energy solution. This study plays a pivotal role in guiding governments and key stakeholders toward fulfilling the Paris Agreement and advancing the global agenda for Sustainable Development Goal 7. It promotes bold, forward-looking strategies to tackle pressing energy issues, aiming to deliver universal access to clean, affordable energy by 2030 and fast-track the shift to net-zero emissions by 2050.

This study investigates four potential grid-connected HRES configurations for a regional area in Australia, aiming to achieve zero CO_2 emissions by 2050 in line with national renewable energy targets—38 % by 2024, 50 % by 2030, 70 % by 2040, and 90 % by 2050. This research evaluates a range of energy sources, storage technologies, and economic factors to identify the most cost-effective, technically feasible, and environmentally sustainable solution. A unique aspect of this work is the integration of hydrogen storage and Li-ion batteries into a hybrid energy storage system (HESS), designed to support both daily load balancing and long-term energy needs. The study also incorporates electric mobility loads, including electric vehicles (EVs) and hydrogen fuel cell vehicles, to reflect evolving energy demand profiles. Unlike prior studies focused on isolated technologies, this research offers a holistic, future-oriented modeling approach across 2024–2050, accounting for local renewable resource availability, policy-driven transitions, and realistic load growth assumptions. The contributions of this research are outlined as follows.

- Develop a future-oriented scenario-based evaluation (2024–2050) of a net-zero pathway for regional communities based on the availability of local renewable energy resources, emphasizing optimal sizing and system design.
- Develop an integrated modelling of EVs, H_2 production, and grid interactions.
- Design a hybrid energy storage system (HESS) that combines hydrogen and Li-ion batteries to meet daily load demands and provide long-term energy storage reliably.
- Develop an optimized HRES framework delivering a reliable, affordable, and environmentally sustainable energy solution for local communities, with a specific focus on minimizing energy costs, reducing carbon footprints, and maximizing renewable fraction (RF).
- Analyze the developed energy system performance from the technical, economic, environmental, and sustainability perspectives.

2. System architectures and modeling

This section outlines the system configurations and mathematical models that define the various components of the HRES.

2.1. System components and configurations

The system aims to meet energy needs for a regional community in developing countries (Australia), targeting cleaner energy use. Australia's renewable energy roadmap, per IEA projections, plans to hit 38 % by 2024, 50 % by 2030, 70 % by 2040, and 90 % by 2050 [22]. The system's goal is to cut CO_2 emissions by reducing diesel and grid reliance while increasing RESs. This marks a major shift toward cleaner energy in the coming decades. Four grid-connected HRES configurations (2024, 2030, 2040, 2050) are modeled to support this shift. The primary components of these systems potentially include PV, WT, BESS, DG, HT, FC, electrolyzer, and converter. A further goal is hydrogen production using RES, which aids in reducing CO_2 emissions and addressing RES intermittency. As shown in Fig. 1, the four configurations share components to support electrical and EV loads, with the hydrogen load profile added for the 2050 scenario.

This study explores the feasibility of an integrated HESS using hydrogen and Li-ion batteries to ensure a reliable electricity supply while reducing CO_2 emissions and managing peak loads efficiently. Fig. 2(a) outlines the techno-economic validation process, assessing operational, technical, economic, and environmental factors. The study considers geographic, meteorological, and economic conditions to confirm the system's viability. Fig. 2(b) illustrates the methodology to achieve NZE in alignment with Australian RF Policy.

2.2. Modelling of PV module

The efficiency of a PV panel is primarily affected by solar irradiance and ambient temperature and is determined by the temperature of the PV cell. The actual temperature of the PV cell is calculated using Eq. (1) [23].

$$T_{Cell} = T_{amb}(t) + H_T\left(\frac{T_{Cell},NOCT - T_{amb},NOCT}{H_{T,NOCT}}\right)\left(1 - \frac{\eta_c}{\tau\alpha}\right) \tag{1}$$

Where, T_{Cell} is the cell temperature of PV [°C], $T_{amb}(t)$ ambient temperature [°C], $T_{Cell},NOCT$ cell temperature at NOCT [25 °C], $T_{amb},NOCT$ ambient temperature at NOCT [20 °C], $H_{T,NOCT}$ solar radiation at NOCT [0.8 kW/m^2], η_c panel efficiency [%], and $\tau\alpha$ solar transmittance and absorptance [0.9].

The PV array's power output is calculated using Eq. (2) [23].

$$P_{PV}(t) = N_{pv}I_{pv}\left(\frac{U_T}{U_{T,STC}}\right)\left[1 + \alpha_p\left(T_{cell} - T_{cell,STC}\right)\right] \tag{2}$$

Where, N_{pv} is the PV array capacity [kW], I_{pv} a derating factor [%], U_T solar radiation (kW/m^2), U_T,STC standard test radiation [1 kW/m^2], α_p power temperature coefficient [%/°C], $T_{cell,STC}$ cell temperature under standard test conditions [25 °C].

2.3. Wind turbine system

The turbine's power output is calculated using Eq. (3) [24]. Where p_{rated} is the rated power [kW], $v(t)$ wind speed [m/s], v_{rated} rated speed [m/s], v_{cut-in} cut-in speed [m/s], and $v_{cut-off}$ cut-off wind speed [m/s].

$$P_{WT}(t) = \begin{Bmatrix} p_{rated}\left(\frac{v^3(t) - v^3_{cut-in}}{v^3_{rated} - v^3_{cut-in}}\right), v_{cut-in} < v(t) < v_{rated} \\ p_{rated}, v_{rated} < v(t) \le v_{cut-off} \\ 0, v(t) \le v_{cut-in} \text{ or } v(t) \ge v_{cut-offi} \end{Bmatrix} \tag{3}$$

The wind speed at the height of the turbine's hub is calculated using the following Eq. (4) [25]. Where, N_{hub} is the hub height (m), N_{anem} anemometer height [m/s], H_{hub} wind speed at the hub height [m/s], H_{anem} anemometer height [m/s], and β power law exponent which varies from 0.10 to 0.25 [24].

$$H_{hub} = H_{anem}\cdot\left(\frac{N_{hub}}{N_{anem}}\right)^{\beta} \tag{4}$$

2.4. Battery storage modeling

In a hybrid system, integrating a battery enhances overall system reliability. A Li-ion is chosen to store and release electrical energy, ensuring a stable power supply. During the charging process, the charge level of the battery bank at a specific time t is determined using Eq. (5) [26].

$$P_{Bat}(t) = P_{Bat}(t-1)\times(1-\sigma) + \left[P_{Gen}(t) - \frac{P_L(t)}{\eta_I}\right]\times\eta_{Bat,C} \tag{5}$$

The battery bank's discharge level at time t is calculated using Eq. (6) [26].

$$P_{Bat}(t) = P_{Bat}(t-1)\times(1-\sigma) - \left[\frac{P_L(t)}{\eta_I} - P_{Gen}(t)\right]\times\eta_{Bat,D} \tag{6}$$

The battery bank charges at time $t-1$ and t is denoted by $P_{Bat}(t-1)$ and $P_{Bat}(t)$, σ is the self-discharge rate, η_I efficiency, $P_L(t)$ load demand, $\eta_{Bat,C}$ charge efficiency, $\eta_{Bat,D}$ battery's discharge efficiency and $P_{Gen}(t)$ total energy production from renewables which is given by Eq. (7) [27].

$$P_{Gen}(t) = N_{PV}P_{PV}(t) + N_{WT}P_{WT}(t) \tag{7}$$

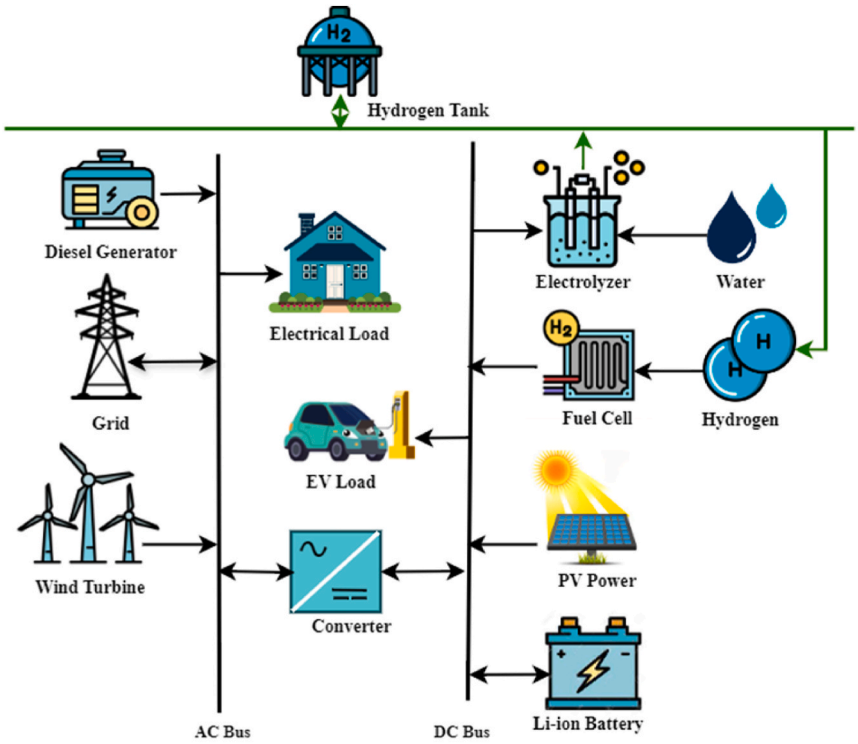

(a)

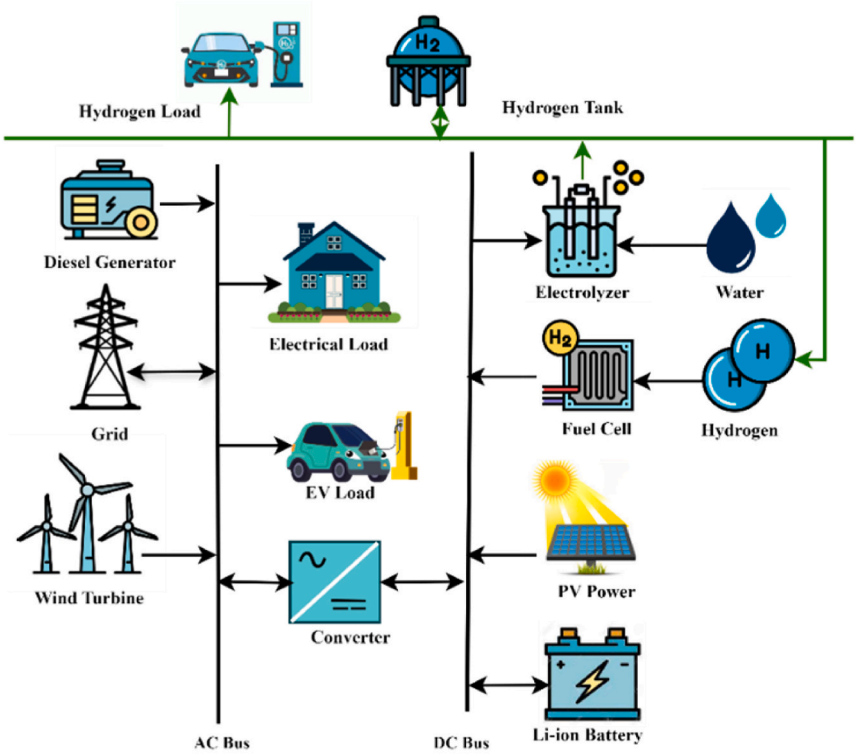

(b)

Fig. 1. The schematic diagram of the suggested energy system (a) for cases 2024, 2030, and 2040, and (b) for case 2050.

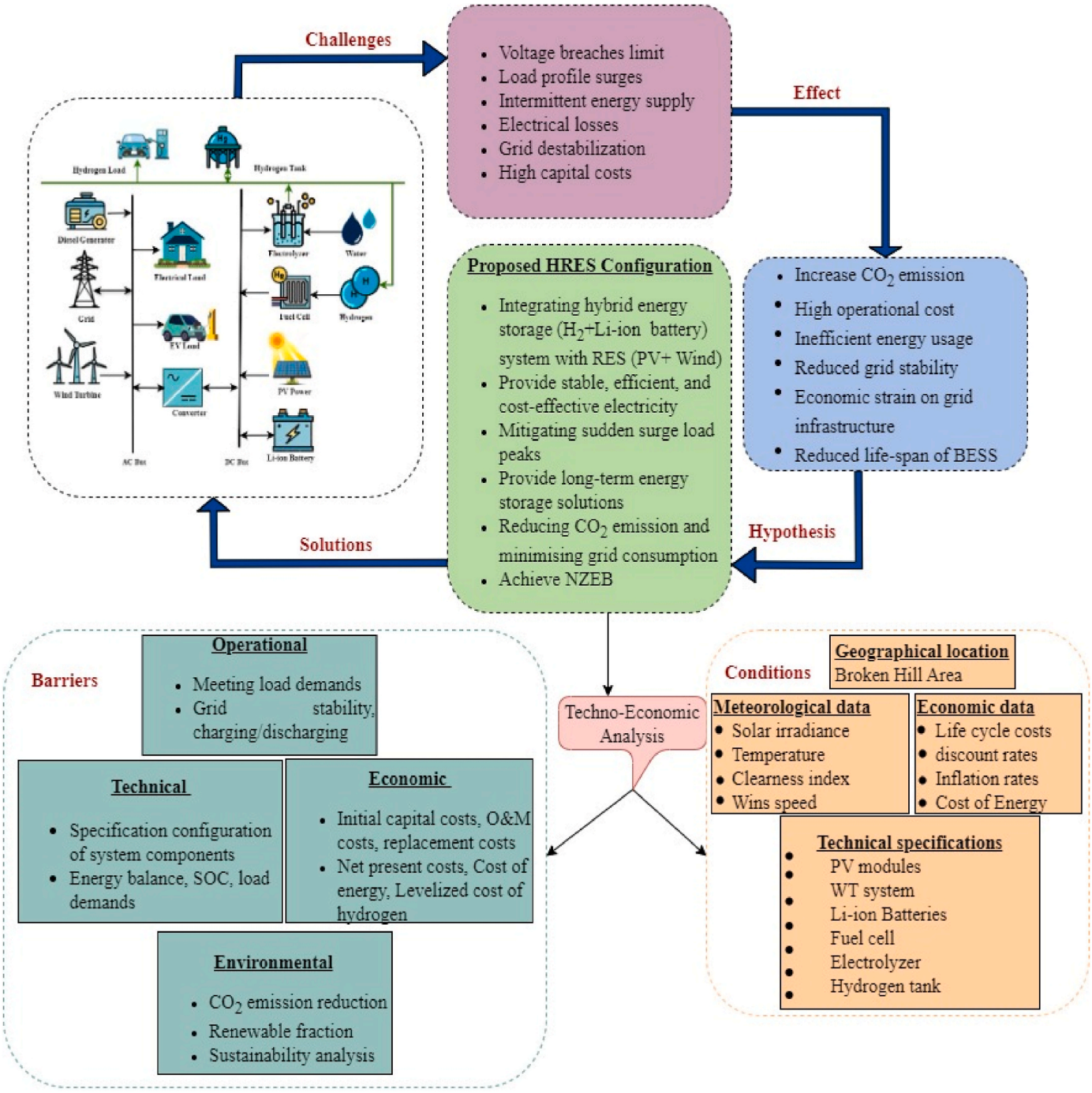

(a)

Fig. 2. (a) Block diagram of the hypothesis of the study, and (b) Strategy to achieve NZE in alignment with Australian RF Policy.

Where, $P_{PV}(t)$ and $P_{WT}(t)$ are the hourly energy generated by PV and wind and N_{PV} and N_{WT} are the number of PV module and WT. The battery charges and discharges within its defined maximum and minimum limits, Eq (8). $P_{Bat,min}$ and $P_{Bat,max}$ is determined using Eqs (9) and (10) [27].

$$P_{Bat,min} \leq P_{Bat}(t) \leq P_{Bat,max} \tag{8}$$

$$P_{Bat,min} = DOD \times P_{nominal} \tag{9}$$

$$P_{Bat,max} = P_{nominal} \tag{10}$$

Where, $P_{nominal}$ represents nominal capacity and DOD depth of discharge.

2.5. Electrolyzer

The mass flow rate of hydrogen production via electrolyzers can be estimated using Eq. (11) [28].

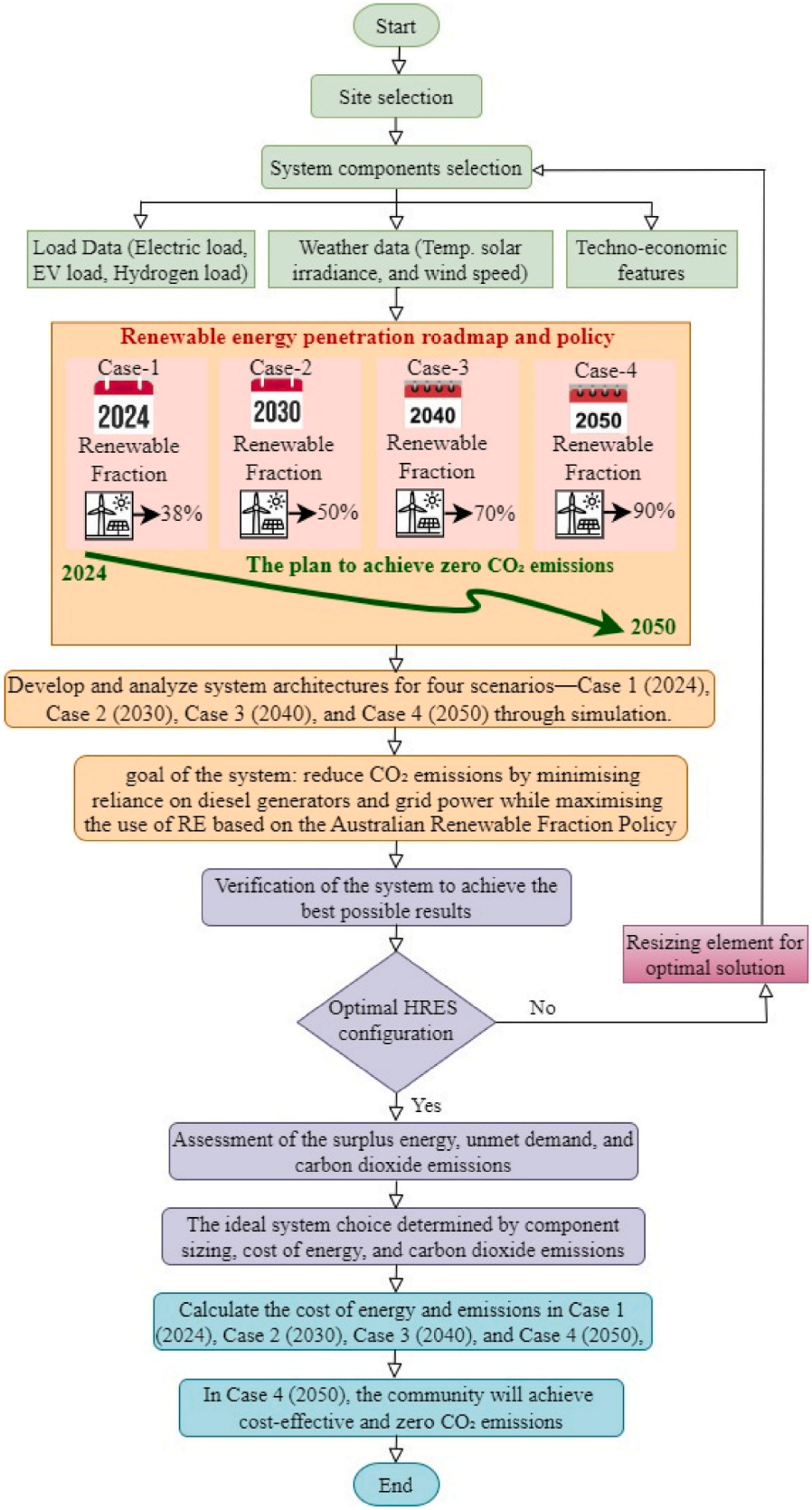

(b)

Fig. 2. (*continued*).

$$MassH_2 = \frac{\eta_{EZ}\, P_{EZ}}{H_{H2}} \tag{11}$$

Where, η_{EZ} denotes the electrolyzer efficiency, H_{H2} heating value [MJ/kg], and P_{EZ} electrical power.

According to Ref. [28], the electrical power of the electrolyzer is defined by Eq. (12), and its nominal power is calculated using Eq. (13).

$$P_{EZ}(t) = \frac{P_{surp}(t)}{\eta_{inv}} \tag{12}$$

$$P_{EZ,n} = \frac{max\{P_{surp}(t)\}}{\eta_{inv}} \tag{13}$$

Where, $P_{surp}(t) = P_{PV}(t) + P_{WT}(t) - P_L(t)$ is the excess power delivered by the PV and wind, being sent to the storage system. η_{inv} is the inverter efficiency.

2.6. Hydrogen tank

In the proposed system, RES first meet the load demand. Any surplus electricity is used to charge the battery, and if additional excess remains, it is directed toward hydrogen production and stored in a hydrogen tank (HT). The tank's capacity is determined using Eq. (14) [28]. Where $LH_2(t)$ denotes the hydrogen load.

$$SOC_{H2}(t) = SOC_{H2}(t-1) + mH_2(t) - LH_2(t) \tag{14}$$

The SOC of the hydrogen tank at a given time t is determined using Eq. (15) [28].

$$SOC_{H2}(t) = SOC_{H2}(t-1) + \frac{P_{EZ}(t).\Delta t.\eta_{EZ}}{C_{H_{2,n}}} - \frac{P_{FC}(t).\Delta t}{\eta_{EZ}.C_{H_{2,n}}} \tag{15}$$

When in operation, the hydrogen tanks must follow the constraints specified in Eq. (16) [29].

$$SOC_{H2-min} \le SOC_{H2}(t) \le SOC_{H2-max} \tag{16}$$

Given that 1 kg of hydrogen equals 39.41 kWh [28], the hydrogen tank's nominal capacity is calculated using Eq. (17). Where, $C_{H_{2-unit}}$ denotes the storage unit capacity of 1 kg and $Coef_{H_{2,n}}$ is the hydrogen tank multiplication factor.

$$C_{H_{2,n}} = Coef_{H_{2,n}} \times C_{H_{2-unit}} \times 39.41 \tag{17}$$

2.7. Fuel cell

In a scenario where the total energy generated from PV, WT, battery storage, and DG is inadequate to meet the needed load demand, such as $P_{PV}(t) + P_{WT}(t) + P_{DG}(t) + P_{bat}(t) < P_{load}(t)$, the FC, generated the further power needed to satisfy the energy necessity for instance $P_{FC}(t) = P_{load}(t) - P_{PV}(t) - P_{WT}(t) - P_{DG}(t) - P_{bat}(t)$.

According to Ref. [28], the instantaneous power output of the FC and the nominal electrical power of the FC are determined by Eqs. (18) and (19). Where, $P_{deficit}(t) = P_{load}(t) - P_{PV}(t) - P_{WT}(t) - P_{DG}(t) - P_{bat}(t)$ is the power produced by the FC when PV, wind, battery, and diesel are unable to meet the load demand; η_{FC} is the efficiency. The fuel cell generates electricity for the system, while the electrolyzer uses surplus power to produce hydrogen.

$$P_{FC}(t) = \frac{P_{deficit}(t)}{\eta_{FC}.\eta_{inv}} \tag{18}$$

$$P_{FC,n}(t) = \frac{max\{P_{deficit}(t)\}}{\eta_{FC}.\eta_{inv}} \tag{19}$$

2.8. Converter system

Bidirectional power converters in hybrid systems manage energy flow between DC and AC buses, functioning as both rectifiers (DC to AC) and inverters (AC to DC). The inverter efficiency (η_{inv}) is determined by the ratio of its output power to its input power, as expressed in the corresponding equation [30].

$$\eta_{inv} = \frac{P_{inv,out}}{P_{DC}} \tag{20}$$

Where, $P_{inv,out}$ refers the inverter's output power [kW], and P_{DC} denotes DC input power [kW].

Similarly, the rectifier's efficiency (η_{rec}) is calculated as the ratio of rectifier output to its input power, as shown in Eq. (21) [30]. $P_{rec,out}$ represents the rectifier's output power [kW], and P_{DC} denotes its AC input power [kW].

$$\eta_{rec} = \frac{P_{rec,out}}{P_{AC}} \tag{21}$$

2.9. Grid modelling

The proposed system is able to buy or sell electricity to the grid. When the PV system and WT fail to meet the electricity demand and the batteries cannot cover the shortfall, the grid steps in to provide the necessary power. The revenue generated from selling spare energy to the utility is calculated using a specific formula [31].

$$R_{grid} = \sum_{t=1}^{8760} \text{rate}_{\text{feed-in tariff}} .P_{grid_{selling}}(t) \tag{22}$$

Where, $\text{rate}_{\text{feed-in tariff}}$ denotes the feed-in tariff rate.

The cost of purchasing electricity from the grid is determined using (23) [31].

$$C_{grid} = C_p \times \sum_{t=1}^{8760} P_{grid_{buying}}(t) \tag{23}$$

Where, C_p refers to the cost per unit of electricity bought from the grid.

2.10. Diesel generator modelling

DG is essential in the hybrid system as a backup source. The hourly fuel consumption of the DG, $F_{DG}(t)$ [L/h], can be expressed linearly relying on the required output power by the load [32].

$$F_{DG}(t) = \gamma_{DG} \times P(t)_{DG generated} + \mu_{DG} \times P_{DG,rated} \tag{24}$$

Where, $P_{DG,rated}$ (kW) and $P(t)_{DG generated}$ (kW) represents the rated power and power generated by the DG, and the fuel consumption curve is determined by coefficients μ_{DG} (L/kWh), and γ_{DG} (L/kWh). Typical values for μ_{DG}, and γ_{DG} are 0.246 and 0.08145 (L/kWh) [32].

The DG efficiency (kW h/L) can be described by the following Eq [32].

$$\eta_{DG} = \left[\frac{P(t)_{DG generated}}{F_{DG}(t)}\right] = \left[\frac{1}{\gamma_{DG} + \mu_{DG} \times \frac{P_{DG,rated}}{P(t)_{DG generated}}}\right] \tag{25}$$

The efficiency percentage based on the lower heating value of gas oil can be represented by the equation [32]. Where, $LHV_{Gas-oil}$ range between 10 and 11.6 kWh/L.

$$\eta_{DG}\% = \left[\frac{P(t)_{DG generated}(kW)}{F_{DG}(t)\left(\frac{L}{h}\right) \times LHV_{Gas-oil}(kWh/L)}\right] \tag{26}$$

3. Optimization framework

This paper focuses on designing an optimized HRES system based on economic, environmental, and sustainability aspects. This study considers the energy management strategy, objective functions, decision variables, and constraints.

3.1. Energy management strategy

The suggested model manages the energy distribution of various technologies PV, Wind, diesel generator, BES, FC, and power grid to effectively satisfy load requirements. It determines the optimal size for each component and ensures effective power flow management. Fig. 3 illustrates the energy and power management flowcharts for grid-connected systems. The control strategy balances energy supply and demand while managing the charging of batteries and hydrogen storage. The operational strategies are founded on the subsequent scenarios.

Case 1. when the total power produced by PV and wind exceeds the load demand ($P_{PV}(t) + P_{WT}(t) > P_{load}(t)$), they first meet electricity needs. Excess energy charges the battery, and any leftover power generates and stores hydrogen in the HT. The FC and diesel generator remain inactive in this scenario.

Case 2. If the electricity from PV and wind exceeds the load, the surplus energy is used to fully charge the BES and hydrogen storage. Any leftover energy is then sent to the grid.

Case 3. If the demand is higher than the PV and wind output, the BES discharges to meet the load. The system prioritizes using PV, wind, and BES to supply electricity.

Case 4. When the combined output from PV, wind, and BES is insufficient to meet demand $P_{PV}(t) + P_{WT}(t) + P_{bat}(t) < P_{load}(t)$, the FC can generate the additional power needed to satisfy the load, i.e., $P_{FC}(t) = P_{load}(t) - P_{PV}(t) - P_{WT}(t) - P_{bat}(t)$.

Case 5. If the combined power output from PV, wind, BES, and FC is

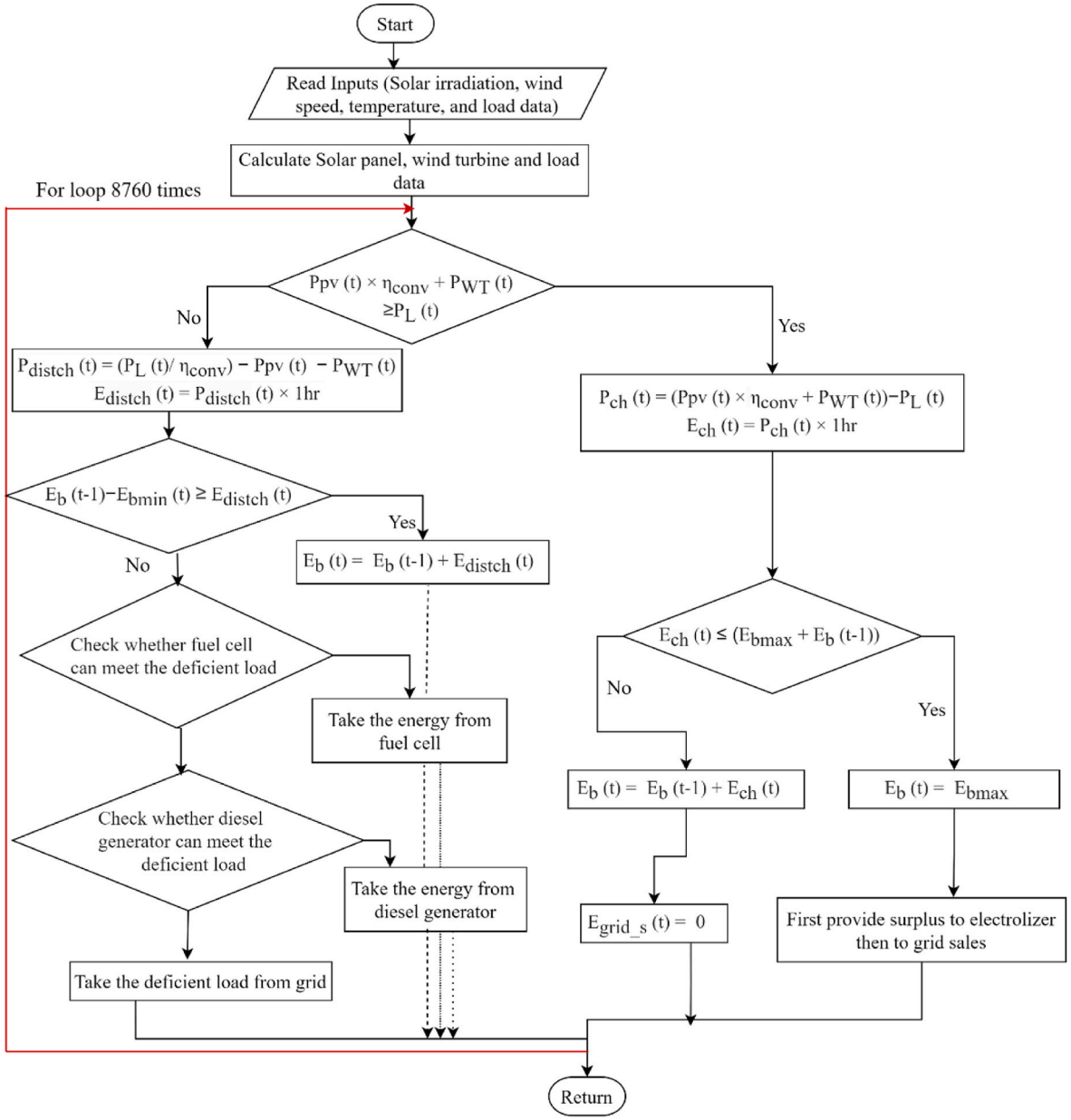

Fig. 3. Flowcharts outlining the energy management strategy for the grid-connected system.

still inadequate $[P_{PV}(t) + P_{WT}(t) + E_{bat}(t) + P_{FC}(t) < P_{load}(t)]$, the DG can supply the remaining power, i.e., $P_{DG}(t) = P_{load}(t) - P_{PV}(t) - P_{WT}(t) - P_{bat}(t) - P_{FC}(t)$

Case 6. If $P_{PV}(t) + P_{WT}(t) + P_{bat}(t) + P_{FC}(t) + P_{DG}(t) < P_{load}(t)$, the system will draw the remaining power from the grid.

Below are the abbreviations used in the flowcharts:

$P_{PV}(t)$: Solar panel power

$P_{WT}(t)$: Power of wind turbine

$P_{ch}(t)$: Power available for charging the battery

$P_{distch}(t)$: Battery discharge power

$\eta_{conv}(t)$: Converter efficiency

$P_{load}(t)$: Power demand

$E_{ch}(t)$: Battery charging energy

$E_{distch}(t)$: Battery discharging energy

E_{bmax} : Battery maximum capacity

$E_b(t)$: Battery state of charge

$E_{grid\_s}(t)$: Energy supplied to the grid

3.2. Objective functions

The objective is to design an optimized HRES system that prioritizes cost efficiency and environmental sustainability. To do so, economic, environmental, and sustainability aspects are evaluated as follows.

Economic aspect:

The first objective function, COE, is calculated using Eq. (27) [26], where TNPC represents the total net present cost, and CRF is the capital recovery factor.

$$Min\ COE = \frac{TNPC \times CRF_{(i_r,N)}}{\sum_{t=1}^{T} E_{loadserved}} \tag{27}$$

The TNPC is calculated in Equation (28), which sums the initial (C_{int}), operational and maintenance ($C_{O\&mai}$), replacement (C_{rep}), fuel (C_{fuel}), and salvage (C_{salv}) costs of the system. More details on these parameters can be found in Ref. [26].

$$TNPC = C_{int} + C_{rep} + C_{fuel} + C_{salv} + C_{O\&mai} + C_{grid} - R_{grid} \tag{28}$$

The CRF depends on the actual interest rate (i_r) and the project lifetime (N), determined by Eq. (29) [33].

$$CRF_{(i_r,N)} = \frac{i_r(1+i_r)^N}{(1+i_r)^N - 1} \tag{29}$$

The actual interest rate is derived from Eq. (30) [26]. $i_r^{\sim}$ and f are the nominal interest rate and annual inflation rate.

$$i_r = \frac{i_r^{\sim} - f}{1+f} \tag{30}$$

Environmental aspect:

The total life cycle emissions (LCE) of the HES over a year are evaluated by Eq. (31) [34]. Here, j_n represents the lifetime equivalent CO_2 emissions, and E_n denotes the energy stored in batteries or converted by system components like PV, WT, Bat, DG, grid, FC, EZ, and Conv to meet demand over T (8760 h).

$$LCE = \sum_{n} \sum_{t=1}^{T} j_n E_{nt}, n \in \{PV, WT, Bat, DG, grid, FC, EZ, Conv\} \tag{31}$$

Sustainability aspect:

The renewable fraction (RF) represents the share of renewable energy used to meet demand, as defined by Eq. (32) [34]. Here, E_{nonren} refers to non-renewable energy used, while $E_{loadserved}$ is the total energy supplied.

$$RF = 1 - \frac{E_{nonren}}{E_{loadserved}} \tag{32}$$

3.3. Constraints and decision variables

In this research, the decision variables include the number of PV modules (N_{PV}), wind turbines (N_{WT}), batteries (N_{Bat}), electrolyzer (N_{Ez}), hydrogen tank (N_{HT}), and fuel cell (N_{FC}). These variables must adhere to the following constraints.

$$N_{PV,min} \le N_{PV} \le N_{PV,max} \tag{33}$$

$$N_{WT,min} \le N_{WT} \le N_{WT,max} \tag{34}$$

$$N_{Bat,min} \le N_{Bat} \le N_{Bat,max} \tag{35}$$

$$N_{EZ,min} \le N_{EZ} \le N_{EZ,max} \tag{36}$$

$$N_{HT,min} \le N_{HT} \le N_{HT,max} \tag{37}$$

$$N_{FC,min} \le N_{FC} \le N_{FC,max} \tag{38}$$

The total hourly energy produced by all system components must meet the hourly load demand.

$$P_{PV}(t) + P_{WT}(t) + P_{bat}(t) + P_{FC}(t) + P_{DG}(t) - P_{grid_{buying}}(t) + P_{grid_{selling}}(t) = P_{load}(t) \tag{39}$$

The capacity of the storage systems must comply with the following constraints.

$$P_{Bat,min} \le P_{Bat}(t) \le P_{Bat,max} \tag{40}$$

$$SOC_{H2-min} \le SOC_{H2}(t) \le SOC_{H2-max} \tag{41}$$

4. Result and discussion

This study seeks to determine the appropriate solution for delivering energy to a regional community. The RESs utilized in this study include PV, WT, FC. Additional components such as electrolyzers, HT, batteries, and converters are utilized for storage or energy conversion purposes. The HS is considered due to its growing popularity as an energy storage solution (ESS), offering advantages like higher energy density, greater efficiency, longer lifespan, and quicker refuelling times, which make it suitable for long-term energy storage solutions. To determine the optimal combination with the available RESs, the study also incorporates the national grid and a DG into the HES. The analysis will explore and discuss the results of the optimal modelling for four scenarios: case 1 (2024), case 2 (2030), case 3 (2040), and case 4 (2050), with a focus on techno-economic, environmental, and sustainability criteria. The simulation and optimization focus on assessing the feasibility of different system configurations, comparing their economic efficiency and environmental impact. To do so, a linear programming framework [35] has been incorporated. The case study presents the system configurations and includes a detailed description below.

4.1. Case 1: Techno-economic evaluation of HES for 2024

In this case, a system integrating PV-WT-DG–HS–LIB-Grid-Converter is modeled and simulated. This configuration includes 33 kW PV, 15 kW WT, 25 kW DG, 32 kWh Li-ion, 20 kW FC, an electrolyser and HT, and a 70-kW converter. The total COE is $0.299/kWh, and the NPC of the system is $960,610. This system has the maximum COE of other systems, which is not optimal among the four case studies. Fig. 4 shows the energy production output of each component during the first seven days of the warmest month (January) and the coldest month (June). The results indicate that most of the time, the grid supplies the load demand rather than renewable sources. When the grid is unavailable, the battery, diesel generator, and FC step in to meet the demand. The DG primarily operates at night when energy consumption peaks. The LIB charges in the morning when there is extra power from the PV and WT, and discharges at night when additional power is needed. According to the simulation result, the developed model has a total consumption of 249,861 kWh/yr, broken down as follows: electric loads for 227,478 kWh/yr, EV load is 16,425 kWh/yr, grid sales amount 99 kWh/yr, and electrolyser consumption 5858 kWh/yr. This system purchased electricity from the grid at 148,142 kWh/yr and sold it to the grid at 99 kWh/yr.

In Fig. 5 (a), most of the energy demand is met by the power grid, with the leftovers supplied by the PV system, WT, DG, and FC. The simulation results indicated an overall annual energy generation of 253,22 kWh/yr, distributed as follows: PV 56,921 kWh/yr, WT 41,599 kWh/yr, DG 4294 kWh/yr, FC 2271 kWh/yr, and grid purchases 148,142 kWh/yr. As presented in Fig. 5 (b), the system's initial installation cost is $342797, while the salvage value is estimated at $221565. The analysis also highlights necessary component replacements: Li-ion batteries after 15 years, WT after 20 years, and PV panels after 25 years. Fig. 5 (c) illustrates that the largest capital investment is needed for the FC module and, afterwards the PV system. Nevertheless, throughout the project, the power grid experiences greater operational expenses than its initial capital outlay.

4.2. Case 2: Techno-economic evaluation of HES for 2030

A HES consisting of PV-WT-DG–HS–LIB-Grid-Converter is designed and simulated for this case study. The system includes a 53 kW PV, 24 kW WT, 25 kW DG, 48 kWh Li-ion, 20 kW FC, an electrolyser and HT, and an 85-kW converter. The system's COE is $0.262/kWh, with an NPC of $1.02 M. The operating cost is $55,102 and the capital cost is $293,831 of the system. Fig. 6 shows the electricity generation for the first seven days of January and June, with 50 % of the load met by the grid and 50 % from renewable sources, ensuring a balanced energy supply. The simulation results indicate an annual energy consumption of 316,674 kWh/yr, distributed as follows: 242,911 kWh/yr for electric loads, 46,538 kWh/yr for EV charging, 7137 kWh/yr for grid sales, and 20,089 kWh/yr for electrolyzer consumption. The system experiences no excess electricity, unmet load, or capacity shortages. Additionally, it purchases 154,759 kWh/yr annually from the grid while selling 7137 kWh/yr back to it. The analysis demonstrates that solar and wind systems contribute more to the energy mix during summer, due to favourable weather and increased wind availability. Consequently, grid electricity purchases are higher in winter, while grid exports peak in the summer and decrease in the winter. The DG, FC, and battery storage systems mainly function as backup power sources. Notably, the DG is used more frequently in winter because of the decreased renewable energy production, underscoring the seasonal reliance on backup power sources when renewable availability is diminished.

Fig. 7 (a) shows that the load demand was equally met by the power grid and renewable energy, with each contributing 50 % to the total power supply. Fig. 7 (b) shows that the overall capital cost of the project is $296,831, with a salvage value of $158,761 at the end of its lifespan. It is also evident that certain components will require replacement over the project's lifespan. Fig. 7 (c) highlights that the FC module requires the most significant capital investment, closely followed by the PV module. However, for the project's lifespan, the operating costs of the power grid system surpass its initial capital expenditure.

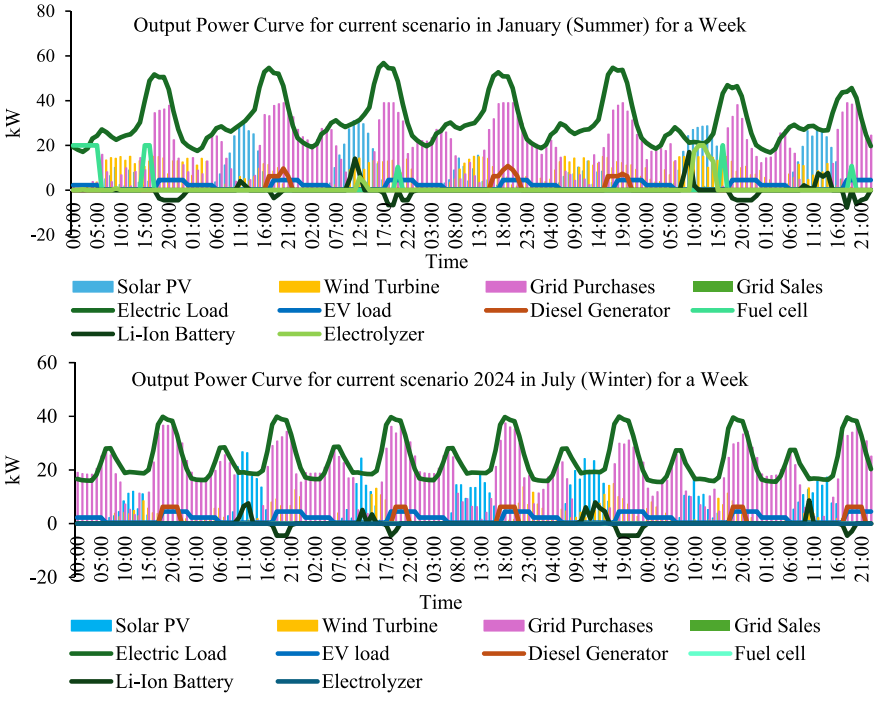

Fig. 4. Output power curve for case 2024 in January (Summer) and July (winter) for a week.

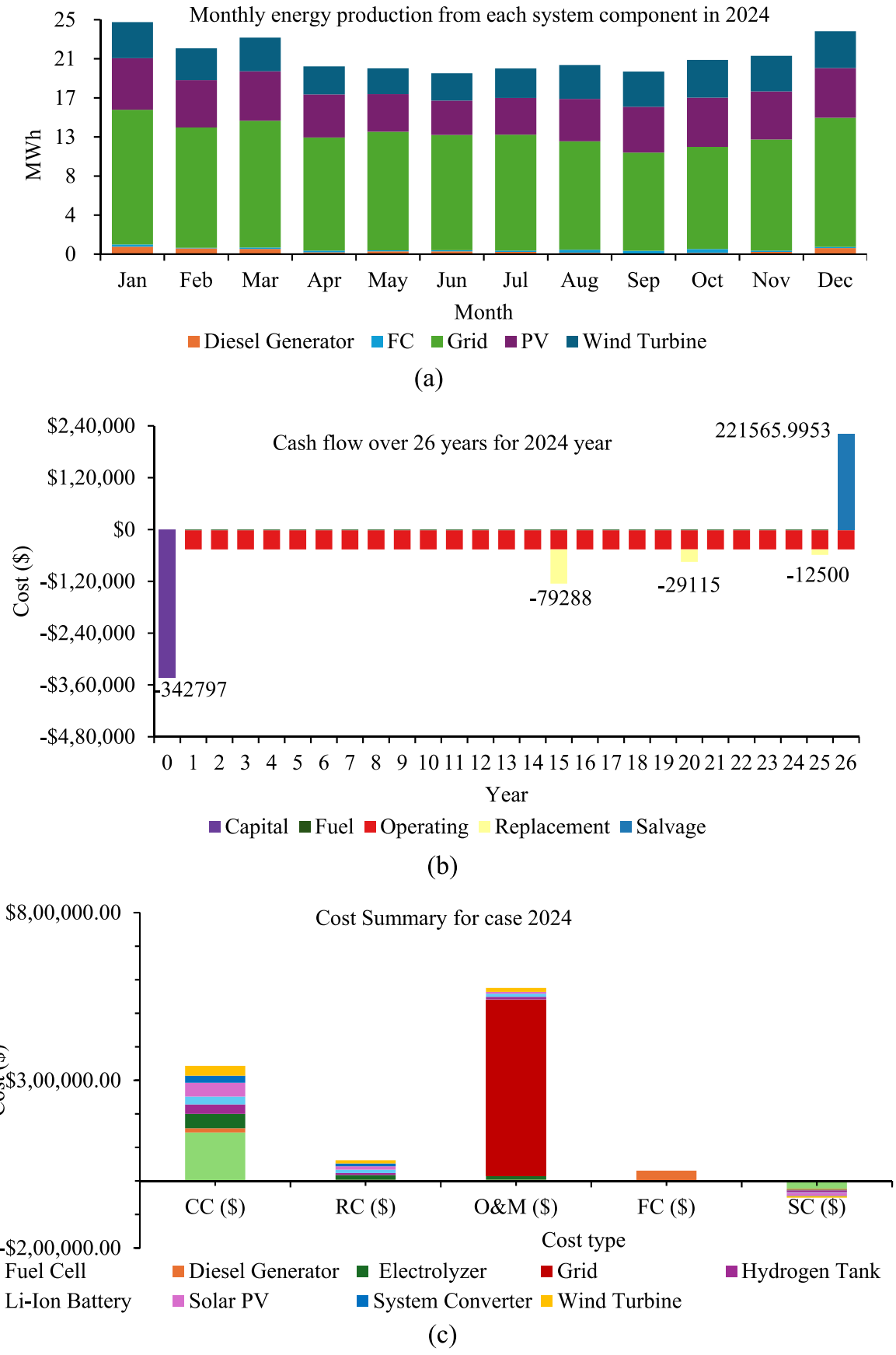

Fig. 5. (a) Monthly energy production from each system component (b) cash flow over 26 years for the current scenario, and (c) summary of annualised costs for 2024.

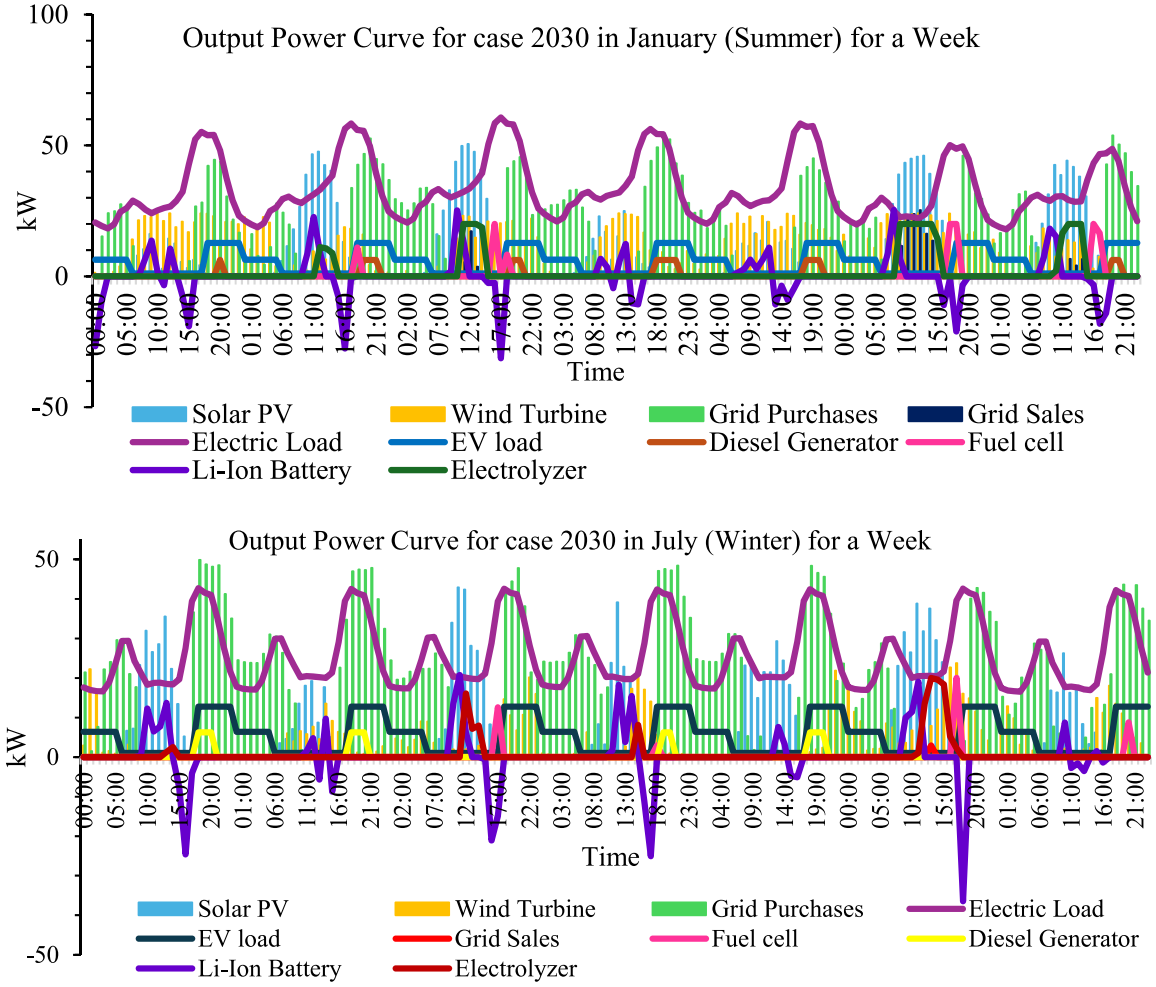

Fig. 6. Output Power Curve for case 2030 in January (Summer) and July (winter) for a Week.

4.3. Case 3: Techno-economic evaluation of HESs for 2040

Case 3 is considered the second most optimal system among the four studied due to its lowest COE of $0.144/kWh and an NPC of $1.10 M. The system's ideal configuration consists of 151 kW PV, 79 kW WT, 25 kW DG, 54 kWh Li-ion, 20 kW FC, an electrolyzer and hydrogen tank, and a 120-kW converter. The developed model's total annual consumption is 643,346 kWh/yr broken down as follows: 270,993 kWh/yr for electric loads, 136,875 kWh/yr for EV loads, 170,663 kWh/yr for grid sales and, 64,815 kWh/yr for electrolyser consumption. The system generates 13,425 kWh/yr of spare electricity, with zero unmet load or capacity shortage. It purchases 168,335 kWh/yr from the grid and exports 170,663 kWh/yr. The output power curve of each component during the first week of the warmest month (January) and the coldest month (June) is illustrated in Fig. 8.

In Fig. 9 (a) most of the power is produced by the PV module and WT, with the remaining power supplied by the grid, FC and diesel generator. Fig. 9 (b) shows that the primary cost of the developed system is $408203 and the salvage cost of the $203070 over the project's lifetime. Replacement costs for the battery, converter, PV, and WT occur in the 10th, 15th, 20th and 25th years, totalling $24,408, $35,040, $118,026 and $95,050 respectively. Fig. 9 (c) illustrates that the largest capital cost is needed for the WT and, subsequently, the PV module. Conversely, the power grid system and WT incur higher operating costs throughout the project. Fuel costs are minimal, which suggests that fuel-dependent components like the DG are not heavily relied on in this scenario. The negative SC suggest the possibility of recovering value from various components once they are decommissioned.

4.4. Case 4: Techno-economic evaluation of HESs for 2050

Case 4 stands out as the most efficient system among the four case studies, featuring the lowest COE of $0.0957/kWh, an NPC of $1.18 million, and producing zero CO2 emissions. The system is designed with a combination of PV, WT, DG, FC, an electrolyzer, HT, battery storage, a bi-directional converter, and grid integration. It includes a 510 kW PV array, 263 kW WT, a 25 kW DG, a 20 kW FC and electrolyzer, a 20 kW HT, a 70-kWh battery, and a 143 kW converter. Peak demand occurs between 6 and 10 p.m. when solar energy is unavailable, and the load is met by WT, battery storage, and the FC. During the day, excess solar energy is first used to charge the battery. If any additional surplus remains, it is directed to hydrogen production, and any further excess is fed into the grid. The total overall consumption of the system is 1,006,473 kWh/yr, distributed as follows: 302,322 kWh/yr for electric loads, 180,675 kWh/yr for EV charging, 68,637 kWh/yr for electrolyzer operation, and 454,840 kWh/yr sold to the grid. The system achieves an excess electricity rate of 42.2 %, with no unmet load. It purchases 106,218 kWh/yr from the grid while selling 454,840 kWh/yr. In summary, Case 4 (2050) offers a reliable, cost-effective, and environmentally friendly solution to meet energy needs. Fig. 10 (a) demonstrates energy production during the hottest month, January, and the coldest month, June. Fig. 10 (b) shows the hydrogen production and consumption profile for Case 2050 in January (summer) and July (winter) for a week. Hydrogen production occurs mainly during the day when

Fig. 7. (a) monthly energy production from each system component (b) cash flow over 26 years for the case of 2030, and (c) summary of annualised costs for 2030.

excess solar energy is converted into hydrogen and stored for nighttime electricity generation through the fuel cell.

Fig. 11 (a) illustrates that most of the energy demand is met by the PV and WT, while the leftover demand is provided by the power grid, FC, and DG. In Fig. 11 (b), it is noted that the initial installation cost of the system is $963,004. Additionally, replacement costs for the WT and solar panel are incurred in the 20th and 25th years of the project, amounting to $384,506 and $255,350, respectively. In years 6th, 12th, 17th and 23rd the Li-ion battery must be replaced, and 14th and 15th also must be replaced FC and converter. Fig. 11 (c) shows the WT and PV modules have the highest capital costs, while the power grid and WT face higher operating costs. Minimal fuel costs indicate limited reliance on fuel-dependent components like the DG. Negative SC suggests potential value recovery from decommissioned components.

Fig. 11 (d) shows COE and NPC for the HRES configuration based on different years. The analysis evaluates four time periods (2024, 2030,

Fig. 8. Output Power Curve for case 2040 in January (Summer) and July (winter) for a Week.

2040, and 2050) to assess their effect on the COE and NPC. From the figure, it is evident that while the NPC fluctuates slightly over time, the COE decreases significantly, especially after 2030. The results show a significant reduction in energy costs, with the COE decreasing from $0.299/kWh in the current scenario to $0.0957/kWh by 2050, demonstrating a highly cost-effective system. Therefore, this study highlights the economic benefits of adopting renewable energy over time, despite the slight increase in NPC. Lod profiles and meteorological resource descriptions including study area, electrical load, electrical vehicle load, and hydrogen vehicle load have been provided in the **Supplementary File.**

4.5. Sensitivity analysis of economic parameters

A comprehensive sensitivity analysis was conducted to assess the impact of capital cost variations on system economics. The capital costs of PV systems, electrolyzers, wind turbines, and fuel cells were individually varied by ±10 % and ±20 % across all future scenarios. The results (summarized in Table 1) show that both LCOE and NPC are moderately to highly sensitive to these changes, especially in the 2040 and 2050 scenarios where hydrogen infrastructure is more dominant. For example, in the 2050 scenario, a 20 % reduction in component costs leads to a 14.9 % decrease in LCOE (from 0.0957 to 0.0815 $/kWh), while a 20 % increase results in a 14.9 % LCOE rise (to 0.110 $/kWh). Similarly, NPC fluctuates by ±15.3 %, from 1.00 M to 1.36 M AUD. These findings underscore the importance of financial incentives and technology cost reductions in achieving economically feasible hydrogen-based hybrid energy systems, particularly in long-term net-zero pathways.

4.6. Environmental and sustainability analysis

The combustion of fossil fuels releases pollutants such as CO_2, CO, SO_2, NO_x, particulate matter, and unburned hydrogen, contributing to air pollution and environmental degradation. The environmental assessment of the HRES focuses on two key factors: CO_2 emissions and RF. A primary goal of the system is to reduce CO_2 emissions by minimizing reliance on diesel generators and grid power while maximizing the use of RES. Fig. 12 (a) presents a radar chart depicting the projected emissions of various pollutants (kg/year) across four time periods: 2024, 2030, 2040, and 2050. The highest CO_2 emissions occur in 2024 (97,952 kg/year) and 2030 (96,997 kg/year). However, emissions decline sharply to 601 kg/year by 2040 and reach zero by 2050, reflecting the increased adoption of renewable energy. Similarly, NO_x

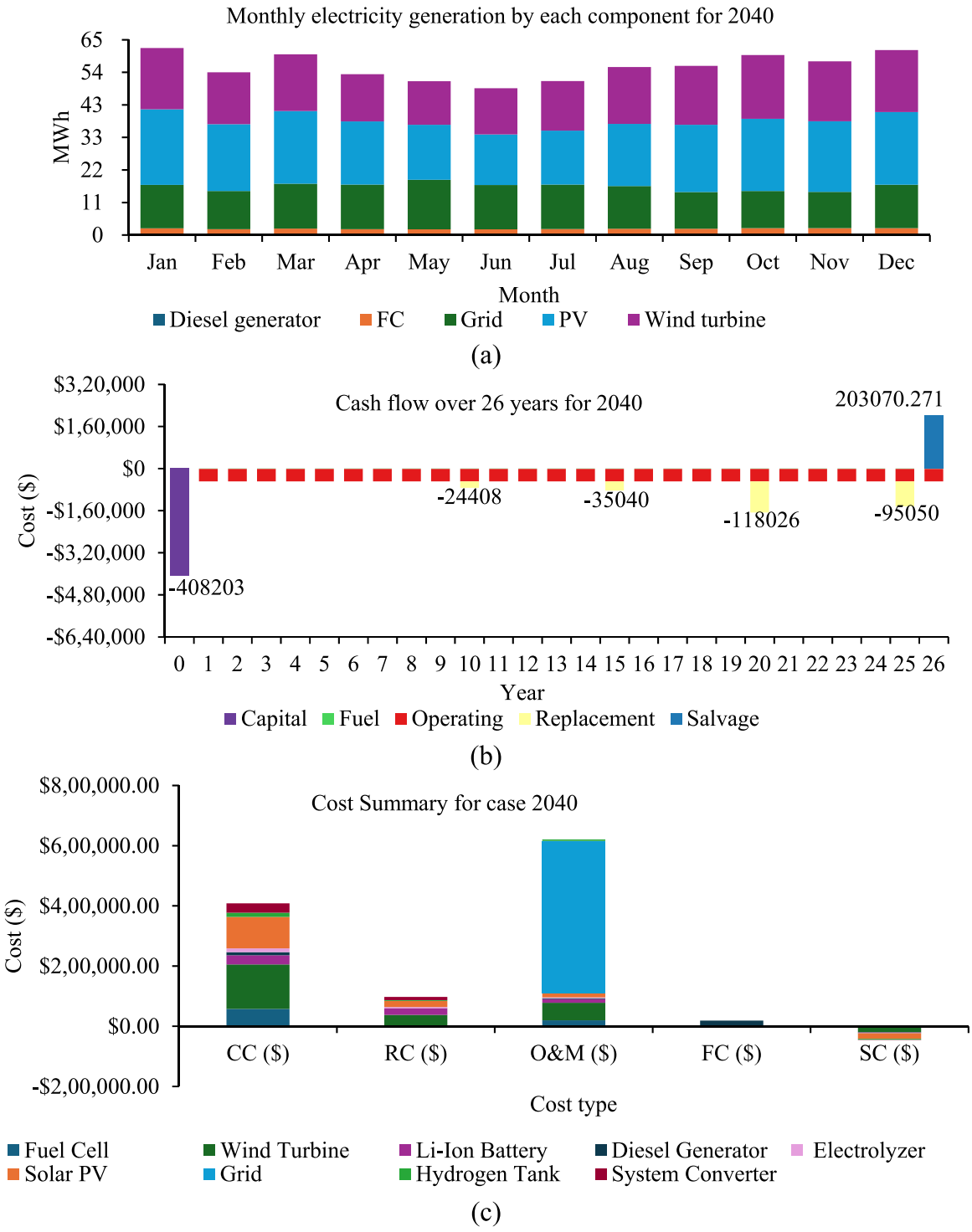

Fig. 9. (a) monthly energy production from each system component (b) cash flow over 26 years for the case 2040, and (c) summary of annualised costs for 2040.

emissions decrease from 245 kg/year in 2024 to 232 kg/year in 2030, dropping significantly to 90.1 kg/year by 2040 and reaching zero by 2050. SO_2 emissions, which remain steady in 2024 (416 kg/year) and 2030 (414 kg/year), also fall to zero by 2040 and 2050, indicating a transition away from fossil fuel-based power generation. The chart highlights the progressive decline in all pollutant emissions by 2050, demonstrating a shift toward cleaner energy technologies. The most significant reductions are observed in CO_2, NO_x, and SO_2 emissions, which are nearly eliminated by 2050. This analysis confirms that the 2050 scenario represents the most environmentally sustainable energy system, achieving zero CO_2 emissions and a higher reliance on RES. However, Negative emissions in HOMER software typically occur when a system generates more low-emission electricity than it consumes and sells the excess to the grid. This reduces the overall grid emissions, and HOMER credits the system with these reductions. If the system's grid sales outweigh its purchases, the net grid emissions can be considered zero, offsetting emissions from conventional grid power sources.

The RF is quite low at the beginning. In 2024, it is approximately 38 %, and by 2030, it grows to around 50 %. Later, the renewable fraction grows even more until it almost reaches 70 % in 2040. By 2050, the RF

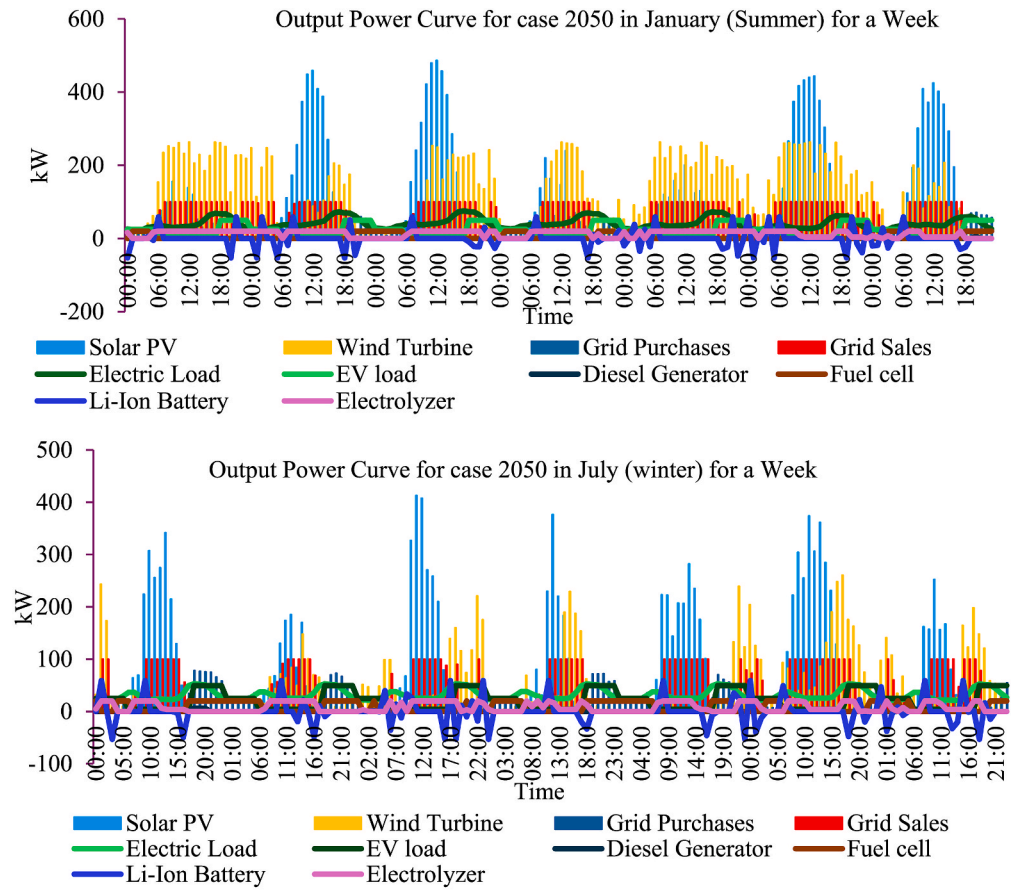

(a)

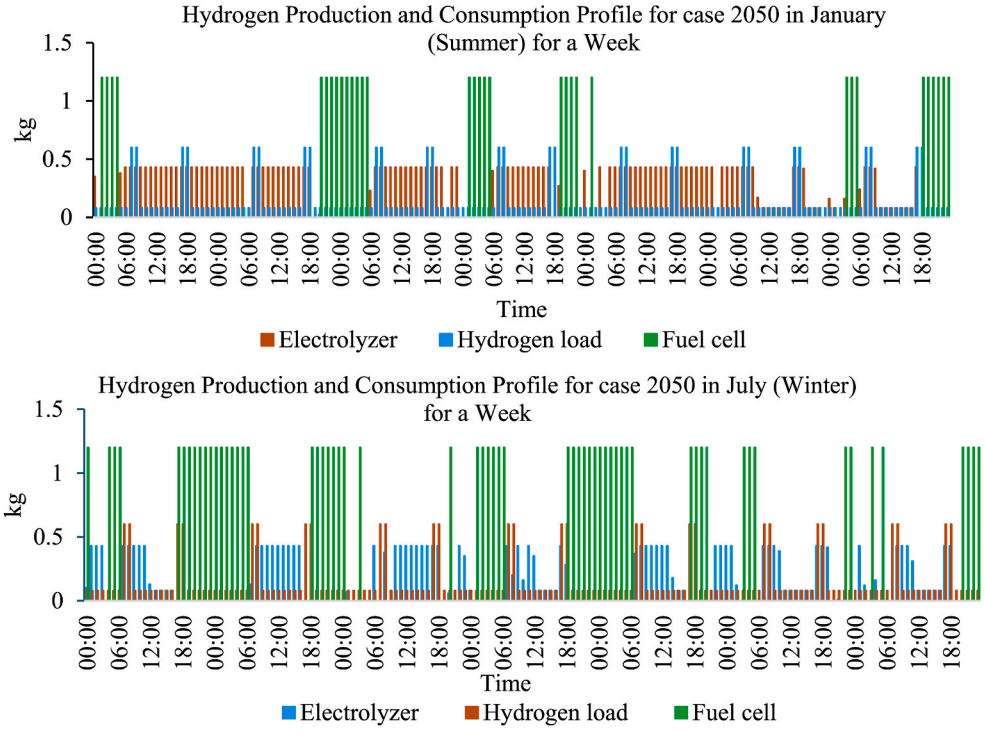

(b)

Fig. 10. (a) Output Power Curve for case 2050 in January (Summer) and July (winter) for a Week (b) hydrogen production and consumption profile for case 2050 case in January (Summer) and July (winter) for a Week.

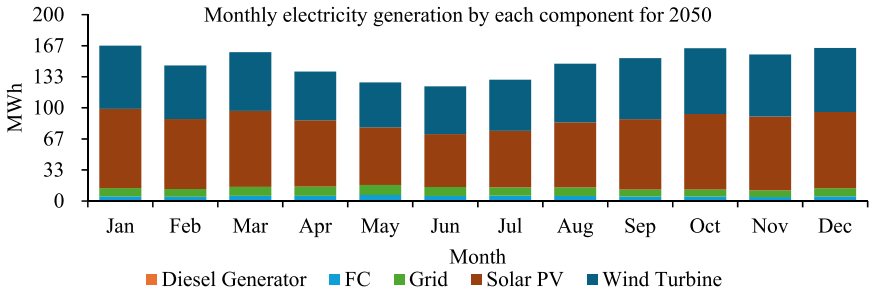

(a)

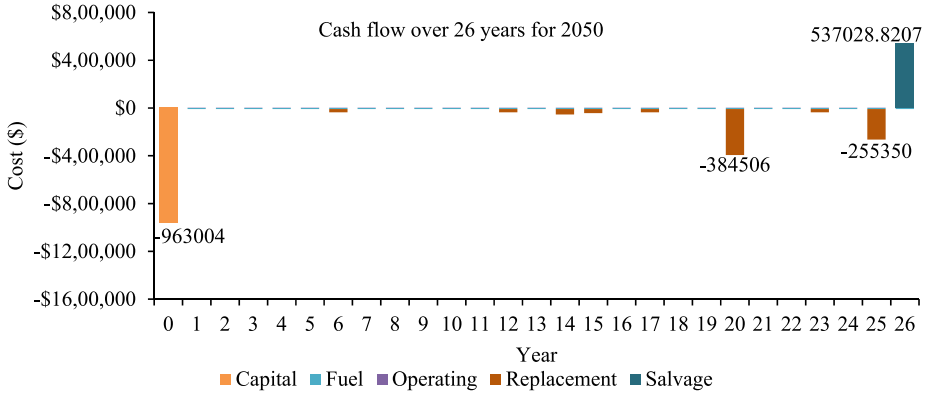

(b)

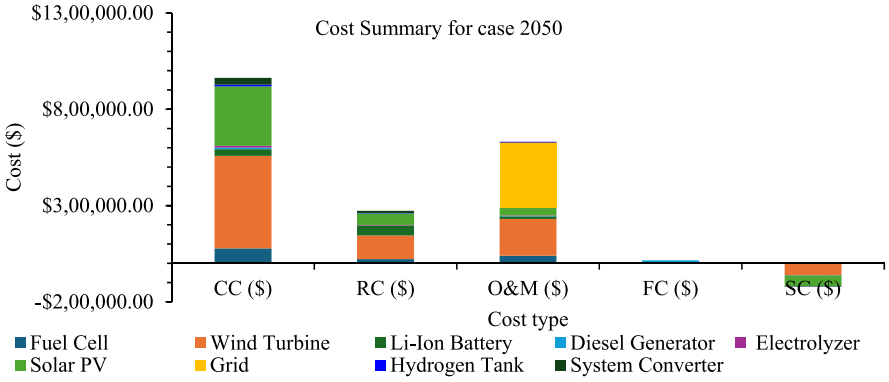

(c)

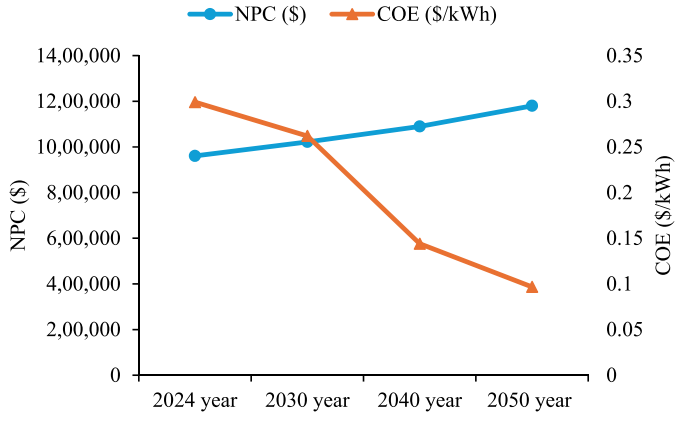

(d)

Fig. 11. (a) monthly energy production from each system component (b) cash flow over 26 years for 2050 (c) summary of annualised costs for 2050, and (d) COE and NPC for the HRES configuration based on different years.

Table 1
Sensitivity analysis of LCOE and NPC to ±20 % Capital Cost Variations.

Year	Technology	Base Case	Scenario 1	Scenario 2	Scenario 3	Scenario 4
	PV	No change	−10 %	−20 %	+10 %	+20 %
	Electrolyzer	No change	−10 %	−20 %	+10 %	+20 %
	wind	No change	−10 %	−20 %	+10 %	+20 %
	FC	No change	−10 %	−20 %	+10 %	+20 %
Case 2024	NPC ($)	960,610	934,882	909,126	986.352	1.01 M
	LCOE ($/kWh)	0.299	0.291	0.283	0.307	0.315
Case 2030	NPC ($)	1.02 M	1.0 M	979923	1.04 M	1.06 M
	LCOE ($/kWh)	0.262	0.257	0.251	0.266	0.273
Case 2040	NPC ($)	1.10 M	1.07 M	1.03 M	1.13 M	1.16 M
	LCOE ($/kWh)	0.144	0.140	0.136	0.149	0.153
Case 2050	NPC ($)	1.18 M	1.09 M	1.00 M	1.27 M	1.36 M
	LCOE ($/kWh)	0.0957	0.0885	0.0815	0.103	0.110

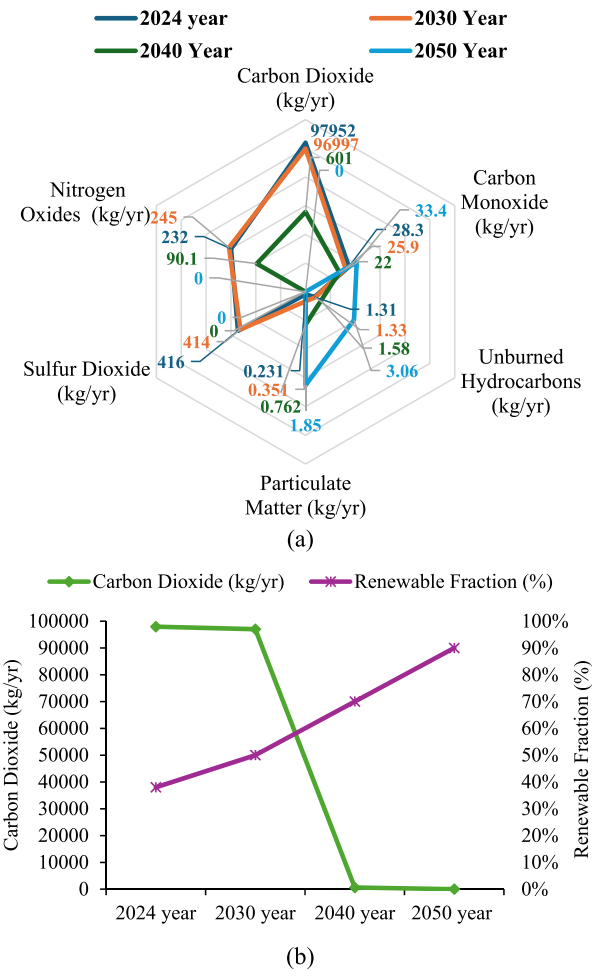

Fig. 12. (a) comparison of pollutant emission for the HRES configuration across different years (b) CO_2 emission and RF for the HRES configuration across different years.

will reach 90 %, indicating that RES almost entirely powers the energy system. Such correlation with a steep fall in CO_2 emissions shows that renewables replace a large proportion of fossil fuel in the energy generation mix. Fig. 12 (b) shows the inverse relationship between CO_2 emissions and the RF over time. As the share of renewable energy increases, CO_2 emissions drastically decrease. An essential decrease happens between 2030 and 2040, when the RF increases significantly, and CO_2 emission dramatically falls. By 2050, the RF will be almost 90 %, while CO_2 production will be eliminated, reflecting the success of the transition to a low-carbon energy system. Comparative analysis has been discussed in the **Supplementary File**.

5. Conclusion

This study conducts a techno-economic analysis of a grid-connected HRES to decide the most suitable configuration for the selected location. The study focuses on the Broken Hill region in far-west New South Wales, Australia. The feasibility assessment was carried out using HOMER software, evaluating four different HRES configurations. A system optimization analysis has been executed to judge technical adaptability, economic viability, and environmental issues for all four configurations. For economic analysis, key parameters included the COE, TNPC, ICC, and operation and maintenance expenses. From a technical perspective, factors such as annual energy generation, consumption, surplus energy, unmet demand, and the renewable energy fraction in kWh per year were considered for each system setup. Since the goal of the research is to look for the best configuration due to environmental impact, the calculation for the emissions of each configuration had to be considered. The key results of this research are outlined here.

- Economic aspect: From the economic perspective, the total COE is $0.299/kWh, and the NPC of the case 2024 year is $960,610. In the case of the 2030 year, the total COE is $0.262/kWh, and the NPC of the system is $1.02 M. In the case of the 2040 year, the COE is $0.144/kWh, and NPC is $1.10 M of the suggested system. In addition, in the last case of the 2050 year, the COE is $0.0957/kWh whereas the NPC is $1.18 M respectively.
- Environmental aspect: From the environmental consequences, the annual equivalent avoided CO_2 emissions tend to occur in 2024 (97,952 kg/yr) and the 2030 scenario (96,997 kg/yr). There is estimated to be a sharp decline of (601 kg/year) in 2040 and (0 kg/yr) in 2050 suggesting a significant decrease in their CO_2 emissions over time.
- Sustainability aspect: From the sustainability perspective, the renewable fraction is quite low at the beginning. In 2024 year, it is approximately 38 %, and by 2030, it grows to around 50 %. Later, the RF grows even more until it almost reaches 70 % in 2040. By 2050, the RF will reach 90 %, indicating that RES almost entirely powers the energy system.

Based on the above explanation, we found that the case 2050 year is optimal system from the technical and economic perspective, and is the superior configuration from the environmental and sustainability

aspect. In the case of 2050 year, more energy can sell to the grid than in other cases. Based on that analysis, Australia can achieve a cost-effective, NZE community by 2050.

In brief, the theoretical contributions are to assess and compare the configurations of the HRES system. By analyzing key parameters such as TNPC, COE, ICC, energy generation and consumption, excess and unmet energy, RE fraction, and GHG emissions, we assessed the economic feasibility, technical performance, and environmental impact of each configuration. The results identified the optimum clean energy generation design, enhancing knowledge in renewable power generation. It also provides relevant insight to decision-makers and other stakeholders who are interested in implementing viable and low-cost energy systems in other regions. Identifying the most efficient and cost-effective HRES setup provides valuable insights for designing and implementing renewable energy projects in the target region. Practical consequences of the paper include its contribution to the wider perspective of sustainability and the decrease of GHG emissions. Integrating HRES with conventional generators and energy storage offers a practical approach to diversifying energy sources by reducing reliance on fossil fuels. This strategy enhances energy security and promotes a more sustainable power supply.

CRediT authorship contribution statement

K. Parvin: Writing – original draft, Visualization, Software, Resources, Methodology, Investigation. **Abbas Tabandeh:** Writing – review & editing, Writing – original draft, Validation, Supervision, Methodology, Conceptualization. **M.J. Hossain:** Writing – review & editing, Supervision, Resources, Methodology, Conceptualization. **M.A. Hannan:** Writing – review & editing, Resources, Conceptualization.

Declaration of competing interest

The authors declare that they have no known competing financial interests or personal relationships that could have appeared to influence the work reported in this paper.

Appendix A. Supplementary data

Supplementary data to this article can be found online at https://doi.org/10.1016/j.ijhydene.2025.150559.

References

[1] https://www.energy.gov.au/publications/australian-energy-statistics-table-o-electricity-generation-fuel-type-2022-23-and-2023 [Accessed on October 22, 2024].
[2] Hassane AI. Techno-economic feasibility of a remote PV mini-grid electrification system for five localities in Chad. Int J Sustain Eng 2022;15(1):179–93. https://doi.org/10.1080/19397038.2022.2101707.
[3] Tabandeh A, Hossain MJ, Khalilpour K, Huang Z. Planning framework for establishment of hydrogen hubs incorporating the path towards net-zero-driven policies. Int J Hydrogen Energy 2024;82:162–80.
[4] Zhang Y, Yu Y. Carbon value assessment of hydrogen energy connected to the power grid. IEEE Trans Ind Appl 2022;58(2):2803–11. https://doi.org/10.1109/TIA.2021.3126691.
[5] Makepeace RW, Tabandeh A, Hossain MJ, Asaduz-Zaman M. Techno-economic analysis of green hydrogen export. Int J Hydrogen Energy 2024;56:1183–92.
[6] Albertus P, Manser JS, Litzelman S. "Long-Duration electricity Storage Applications, Economics, and Technologies,". Cell Press; Jan. 15, 2020. https://doi.org/10.1016/j.joule.2019.11.009.
[7] Tabandeh A, Hossain MJ, Li L. Integrated multi-stage and multi-zone distribution network expansion planning with renewable energy sources and hydrogen refuelling stations for fuel cell vehicles. Appl Energy 2022;319:119242.
[8] Das BK, Hasan M, Das P. Impact of storage technologies, temporal resolution, and PV tracking on stand-alone hybrid renewable energy for an Australian remote area application. Renew Energy Aug. 2021;173:362–80. https://doi.org/10.1016/j.renene.2021.03.131.
[9] Dhundhara S, Verma YP, Williams A. Techno-economic analysis of the lithium-ion and lead-acid battery in microgrid systems. Energy Convers Manag Dec. 2018;177:122–42. https://doi.org/10.1016/j.enconman.2018.09.030.
[10] Zebarjadi M, Askarzadeh A. Optimization of a reliable grid-connected PV-based power plant with/without energy storage system by a heuristic approach. Sol Energy Feb. 2016;125:12–21. https://doi.org/10.1016/j.solener.2015.11.045.
[11] Gharibi M, Askarzadeh A. Technical and economical bi-objective design of a grid-connected photovoltaic/diesel generator/fuel cell energy system. Sustain Cities Soc 2019;50(Oct). https://doi.org/10.1016/j.scs.2019.101575.
[12] Maleki A, Hafeznia H, Rosen MA, Pourfayaz F. Optimization of a grid-connected hybrid solar-wind-hydrogen CHP system for residential applications by efficient metaheuristic approaches. Appl Therm Eng 2017;123:1263–77. https://doi.org/10.1016/j.applthermaleng.2017.05.100.
[13] González A, Riba JR, Rius A, Puig R. Optimal sizing of a hybrid grid-connected photovoltaic and wind power system. Appl Energy Sep. 2015;154:752–62. https://doi.org/10.1016/j.apenergy.2015.04.105.
[14] Ramli MAM, Hiendro A, Sedraoui K, Twaha S. Optimal sizing of grid-connected photovoltaic energy system in Saudi Arabia. Renew Energy Mar. 2015;75:489–95. https://doi.org/10.1016/j.renene.2014.10.028.
[15] Jahangiri M. Techno-econo-environmental optimal operation of grid-wind-solar electricity generation with hydrogen storage system for domestic scale, case study in Chad. Int J Hydrogen Energy Nov. 2019;44(54):28613–28. https://doi.org/10.1016/j.ijhydene.2019.09.130.
[16] Akram U, Khalid M, Shafiq S. Optimal sizing of a wind/solar/battery hybrid grid-connected microgrid system. IET Renew Power Gener Jan. 2018;12(1):72–80. https://doi.org/10.1049/iet-rpg.2017.0010.
[17] Li C. Techno-economic and environmental evaluation of grid-connected and off-grid hybrid intermittent power generation systems: A case study of a mild humid subtropical climate zone in China. Energy 2021;230(Sep). https://doi.org/10.1016/j.energy.2021.120728.
[18] Basu S, John A, Akshay, Kumar A. Design and feasibility analysis of hydrogen based hybrid energy system: A case study. Int J Hydrogen Energy Oct. 2021;46(70):34574–86. https://doi.org/10.1016/j.ijhydene.2021.08.036.
[19] Ma WW, Rasul MG, Liu G, Li M, Tan XH. Climate change impacts on techno-economic performance of roof PV solar system in Australia. Renew Energy Apr. 2016;88:430–8. https://doi.org/10.1016/j.renene.2015.11.048.
[20] Ali L, Shahnia F. Determination of an economically-suitable and sustainable standalone power system for an off-grid town in Western Australia. Renew Energy 2017;106:243–54. https://doi.org/10.1016/j.renene.2016.12.088.
[21] Uddin M, Mo H, Dong D, Elsawah S. Techno-economic potential of multi-energy community microgrid: The perspective of Australia. Renew Energy 2023;219(Dec). https://doi.org/10.1016/j.renene.2023.119544.
[22] Energy Agency I. Net Zero by 2050 - a roadmap for the global energy sector. www.iea.org/t&c/; 2025.
[23] Jahangir MH, Shahsavari A, Vaziri Rad MA. Feasibility study of a zero emission PV/Wind turbine/Wave energy converter hybrid system for stand-alone power supply: a case study. J Clean Prod 2020;262(Jul). https://doi.org/10.1016/j.jclepro.2020.121250.
[24] Tabandeh A, Hossain MJ. Hybrid scenario-IGDT-based congestion management considering uncertain demand response firms and wind farms. IEEE Syst J 2022;16(Jun). https://doi.org/10.1109/JSYST.2021.3104248.
[25] Baghaee HR, Mirsalim M, Gharehpetian GB, Talebi HA. Reliability/cost-based multi-objective Pareto optimal design of stand-alone wind/PV/FC generation microgrid system. Energy Nov. 2016;115:1022–101. https://doi.org/10.1016/j.energy.2016.09.007.
[26] Das BK, Tushar MSHK, Hassan R. Techno-economic optimisation of stand-alone hybrid renewable energy systems for concurrently meeting electric and heating demand. Sustain Cities Soc May 2021;68. https://doi.org/10.1016/j.scs.2021.102763.
[27] Kaabeche A, Ibtiouen R. Techno-economic optimization of hybrid photovoltaic/wind/diesel/battery generation in a stand-alone power system. Sol Energy May 2014;103:171–82. https://doi.org/10.1016/j.solener.2014.02.017.
[28] Falama RZ, Saidi AS, Souloukngа MH, Ben Salah C. A techno-economic comparative study of renewable energy systems based different storage devices. Energy 2023;266(Mar). https://doi.org/10.1016/j.energy.2022.126411.
[29] Mehrjerdi H. Off-grid solar powered charging station for electric and hydrogen vehicles including fuel cell and hydrogen storage. Int J Hydrogen Energy May 2019;44(23):11574–83. https://doi.org/10.1016/j.ijhydene.2019.03.158.
[30] Li C. Techno-economic and environmental evaluation of grid-connected and off-grid hybrid intermittent power generation systems: a case study of a mild humid subtropical climate zone in China. Energy 2021;230(Sep). https://doi.org/10.1016/j.energy.2021.120728.
[31] Barakat S, Ibrahim H, Elbaset AA. Multi-objective optimization of grid-connected PV-wind hybrid system considering reliability, cost, and environmental aspects. Sustain Cities Soc 2020;60(Sep). https://doi.org/10.1016/j.scs.2020.102178.
[32] Dufo-López R. Multi-objective optimization minimizing cost and life cycle emissions of stand-alone PV-wind-diesel systems with batteries storage. Appl Energy 2011;88(11):4033–41. https://doi.org/10.1016/j.apenergy.2011.04.019.
[33] Adoum Abdoulaye M, Waita S, Wabuge Wekesa C, Mwabora JM. Optimal sizing of an off-grid and grid-connected hybrid photovoltaic-wind system with battery and fuel cell storage system: a techno-economic, environmental, and social assessment. Appl Energy 2024;365(Jul). https://doi.org/10.1016/j.apenergy.2024.123201.
[34] Das P, Das BK, Rahman M, Hassan R. Evaluating the prospect of utilizing excess energy and creating employments from a hybrid energy system meeting electricity and freshwater demands using multi-objective evolutionary algorithms. In: Energy. Elsevier Ltd; Jan. 2022. https://doi.org/10.1016/j.energy.2021.121860.
[35] Tabandeh A, Abdollahi A, Rashidinejad M. Transmission congestion management considering Uncertainty of demand response resources' participation. J Electr Comput Eng Innovat 2015;3(2):77–88. https://doi.org/10.22061/jecei.2016.400.